THE ASTROPHYSICAL JOURNAL, 503:593–598, 1998 August 20
© 1998. The American Astronomical Society. All rights reserved. Printed in U.S.A.

DISCOVERY OF X-RAY EMISSION FROM THE DISTANT LENSING CLUSTER OF GALAXIES Cl 2236−04 AT $z = 0.552$

MAKOTO HATTORI,[1,2,3] HIDEYUKI MATUZAWA,[3,4] KOHJI MORIKAWA,[1] JEAN-PAUL KNEIB,[5] KAZUYUKI YAMASHITA,[6] KAZUYA WATANABE,[7] HANS BÖHRINGER,[2] AND TAKESHI G. TSURU[8]

Received 1997 November 25; accepted 1998 March 26

ABSTRACT

X-ray emission from the distant lensing cluster Cl 2236−04 at $z = 0.552$ was discovered by *ASCA* and *ROSAT*/HRI observations. If the spherical symmetric mass distribution model of the cluster is assumed, the lensing estimate of the cluster mass is a factor of 2 higher than that obtained from X-ray observations as reported for many distant clusters. However, the elliptical and clumpy lens model proposed by Kneib and coworkers is surprisingly consistent with the X-ray observations, assuming that the X-ray–emitting hot gas is isothermal and in a hydrostatic equilibrium state. The existence of the cooling flow in the central region of the cluster is indicated by the short central cooling time and the excess flux detected by *ROSAT*/HRI compared to the *ASCA* flux. However, it is shown that, even if the Cl 2236−04 has a cooling flow in the central region, the temperature measured by *ASCA*, which is the mean emission-weighted cluster temperature in this case, should not be different from the virial temperature of the cluster. Therefore, we conclude that the effects of the clumpiness and nonzero ellipticity in the mass distribution of the cluster are essential to explain the observed feature of the giant luminous arc, and in this cluster there is no discrepancy between strong lensing and X-ray estimation of the cluster mass.

Subject headings: galaxies: clusters: individual (Cl 2236−04) — gravitational lensing — X-rays: galaxies

1. INTRODUCTION

It is one of the prime objectives in observational cosmology to determine mass distributions and total masses of clusters of galaxies at various redshifts. It provides a clue to constrain the unknown cosmological parameters: the species of dark matter, the nature of cosmological mass density fluctuations, the average density in the universe, and the cosmological constant.

Recently, gravitational lensing has become a powerful tool to measure the mass distribution in clusters. Strong lensing events, such as multiple images and/or giant luminous arcs, make it possible to model the central region of clusters. However, many clusters show a mass discrepancy with a total mass deduced from a strong lensing observation being larger by a factor of 2–3 than that deduced from X-ray observations (Loeb & Mao 1994; Miralda-Escudé & Babul 1995; Kneib et al. 1995; Schindler et al. 1995, 1997; Wu & Fang 1997; Ota, Mitsuda, Fukazawa 1998). However, there are some clusters whose masses deduced in these two ways agree very well. In such cases, the multiphase of the intracluster gas (Allen, Fabian, & Kneib 1996; Allen 1998) or asymmetric mass distribution (Piere et al. 1996; Böhringer et al. 1998) has been taken into account in the lens modeling. This indicates that careful studies for a large number of clusters are necessary before reaching the conclusion that the lens modeling gives higher mass estimation than that from X-rays.

Cl 2236−04 was discovered by Melnick et al. (1993) with a giant luminous arc. The redshift of the arc was measured to be $z_{\rm arc} = 1.116$ (Melnick et al. 1993), confirming the gravitational lens picture very satisfactorily. The arc is rather straight, and a velocity structure across the arc is measured (Melnick et al. 1993). These factors give strict constraints on the lensing mass estimation. Further, Cl 2236−04 is one of the best and rarest clusters at high redshift of $z > 0.5$ for which comparison of the mass distribution deduced by two individual methods is possible. We have performed the first deep *ASCA* and *ROSAT*/HRI pointing observations toward Cl 2236−04. In this paper, we report the discovery and the properties of X-ray emission from Cl 2236−04, and the mass distribution deduced from the X-ray observation is compared to the lensing mass.

2. X-RAY OBSERVATIONS

2.1. *ASCA Observation*

We performed an *ASCA* observation of Cl 2236−04 in 1995 June with an effective exposure time of about 40 ks. A new X-ray source was discovered in the direction of Cl 2236−04 with more than 10 σ significance (hereafter referred to as AX J2239−0429). The X-ray source count rate is 4×10^{-3} counts s^{-1} for each gas imaging spectrometer (GIS) and 6×10^{-3} counts s^{-1} for each solid imaging spectrometer (SIS). The X-ray peak position of the source is $(\alpha, \delta)_{2000} = (22^{\rm h}39^{\rm m}32^{\rm s}, -4^{\rm d}30^{\rm m})$ (J2000). This is consistent with the position of the cD galaxy, $(\alpha, \delta)_{2000} = (22^{\rm h}39^{\rm m}32^{\rm s}.767, -4^{\rm d}29^{\rm m}32^{\rm s}.24)$ within the *ASCA* position determination accuracy of $(\Delta\alpha, \Delta\delta) = (\pm 4^{\rm s}, \pm 1^{\rm m})$.

[1] Astronomical Institute, Tôhoku University, Aoba, Sendai 980-77, Japan; hattori@astr.tohoku.ac.jp, morikawa@astr.tohoku.ac.jp.
[2] Max-Planck-Institut für extraterrestrische Physik, Giessenbachstrasse, 85740 Garching, Germany.
[3] The Institute of Physical and Chemical Research (Riken), Hirosawa Wako, Saitama 351-01, Japan.
[4] Miyazaki Prefectural Nursing University, Gujibun Komogasako Otsu 2203, Miyazaki 880, Japan; matuzawa@astro.miyazaki-u.ac.jp.
[5] Observatoire Midi-Pyrénées, Laboratoire d'Astrophysique, UMR 5574, 14 Avenue Edouard Belin, F-31400 Toulouse, France; kneib@obs-mip.fr.
[6] Information Processing Center, Chiba University, Chiba 263, Japan; yamasita@tanpopo.ipc.chiba-u.ac.jp.
[7] Department of Physics, Niigata University, Igarashi, Niigata 950-2102, Japan; kazuya@astro.sc.niigata-u.ac.jp.
[8] Department of Physics, Kyoto University, Sakyo-ku, Kyoto, Japan; tsuru@cr.scphys.kyoto-u.ac.jp.

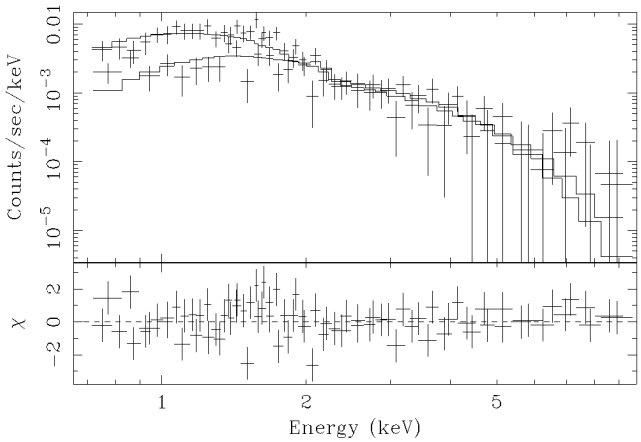


FIG. 1.—X-ray spectra of AX J2239−0429 obtained by *ASCA*. The *ASCA* observatory has four identical telescopes covering the energy range of 0.3–10 keV (Tanaka et al. 1994). They are equipped with two gas imaging spectrometers (GIS 2 and 3) and two solid imaging spectrometers (SIS 0 and 1) at the focal plane. The solid lines are the best-fit Raymond-Smith models obtained by simultaneous fitting of the GIS and SIS spectra.

Figure 1 shows the X-ray spectra of AX J2239−0429 obtained by *ASCA* GIS 2 and 3 and SIS 0 and 1. The SIS data were taken in 2 CCD faint mode. The background for GIS spectrum is taken from blank field observations during the performance verification phase of the *ASCA* mission, wherein point sources contaminating the background spectrum were masked out. The background for the SIS spectrum is taken from the same observation with masking of the source region. Assuming that the source is a cluster of galaxies at $z = 0.552$, the spectrum can be fitted with a Mewe model modified by Galactic absorption. We fixed the hydrogen column density of the Galactic absorption to $N_{\rm H} = 3.87 \times 10^{20}$ cm^{-2} (Dickey & Lockman 1990). The best-fit result with a thermal plasma model is summarized in Table 1. Since the source extent is small and is identical to the point source for *ASCA*, all photons fall into our selected region, and we do not have to worry about the energy-dependent *ASCA* point-spread function (PSF) effect in the analysis (Takahashi et al. 1995). The 2–10 keV band X-ray luminosity, which is estimated from the above best-fit values, is $4.9 \times 10^{44}\ h_{50}^{-2}$ ergs s^{-1}. However, a single power-law model also gives an acceptable fit. The best-fit results are summarized in Table 2. The best-fit photon index of 1.8 is typical of active galactic nuclei (AGNs). Therefore, one cannot distinguish whether the source is a cluster or an AGN.

2.2. *ROSAT*/HRI Observation

The *ROSAT*/HRI observation of Cl 2236−04 was performed in 1996 December with an exposure time of 47 ks. A diffuse source was detected at the position of the cluster Cl 2236−04. The background-subtracted source count within a concentric circle centered on the X-ray peak emission increases monotonically up to 1.′4, and it is 481 ± 43 source counts within a circle of radius 1.′4, which yields a source count rate of $(1.0 \pm 0.1) \times 10^{-2}$ counts s^{-1}, where errors are 1 σ Poisson error. There is no other source with higher than 3 σ detection significance within a circle of radius 3′ centered on the cD. Therefore, we conclude that this source is identical to AX J2239−0429. The HRI count rate is a factor of 1.4 higher than that expected from the *ASCA* observation, that is, $\sim 7 \times 10^{-3}$ counts s^{-1}. Figure 2 shows the source image obtained by *ROSAT*/HRI superposed on the optical image of Cl 2236−04 obtained by the ESO 3.6 m (Melnick et al. 1993). The maximum of the X-ray emission is consistent with the position of the cD galaxy within the HRI pointing accuracy of a few arcseconds.

Figure 3 shows the background-subtracted radial profile of AX J2239−0429 obtained by *ROSAT*/HRI. The radial profile is fitted to a so-called isothermal β model:

$$S_{\rm X}(\theta) = S_0\left(1 + \frac{\theta^2}{\theta_c^2}\right)^{-3\beta+(1/2)}, \qquad (1)$$

where θ_c is angular core radius; best-fit parameters are summarized in Table 3. The source is clearly more extended than the PSF profile. Therefore, we conclude that AX J2239−0429 is X-ray emission from the cluster of galaxies Cl 2236−04. This is the first X-ray detection from the cluster. Because redshift measurement has been done only for a few member galaxies, the X-ray detection confirms that Cl 2236−04 is a real, gravitationally-bound entity. In Table 4, the total gas mass and the total gravitational mass as calculated below are summarized. The gas mass fraction is a typical value.

The central electron number density gives a cooling time of 3.6 Gyr (from eq. [5.23] of Sarazin 1986), which is about half the age of the universe at $z = 0.552$. This short cooling time and the higher count rate of *ROSAT*/HRI compared to *ASCA* may be a signature of cooling flow. The cooling radius where the cooling time equals the age of the universe

TABLE 1

ASCA SPECTRAL FITTING RESULTS WITH A THERMAL PLASMA MODEL

$k_{\rm B}T_{\rm X}$ (keV)	$Z_{\rm Fe}$ ($Z_\odot$)	$N_{\rm H}$ (10^{20} cm^{-2})	z	χ^2 per Degree of Freedom
$6.2^{+2.6}_{-1.7}$.....	$0.0^{+0.38}_{-0.0}$	3.87[a]	0.552[a]	72.66/80 = 0.94

NOTE.—Errors are 90% confidence for one interesting parameter.

[a] Fixed.

TABLE 2

ASCA SPECTRAL FITTING RESULTS WITH A POWER-LAW MODEL

Photon Index	$N_{\rm H}$ (10^{20} cm^{-2})	χ^2 per Degree of Freedom
$1.81^{+0.15}_{-0.15}$.....	3.87[a]	75.00/80 = 0.96

[a] Fixed.

TABLE 3

X-RAY PROPERTIES OF AX J2239−0429 FROM THE SPATIAL ANALYSIS OF *ROSAT*/HRI DATA

S_0 (count s^{-1} arcsec^{-2})	θ_c (arcsec)	β	χ^2 per Degree of Freedom
$1.10^{+0.30}_{-0.25} \times 10^{-5}$.....	$11.39^{+5.5}_{-3.4}$ 84.2 h_{50}^{-1} kpc	$0.66^{+0.22}_{-0.11}$	67.665/56 = 1.21

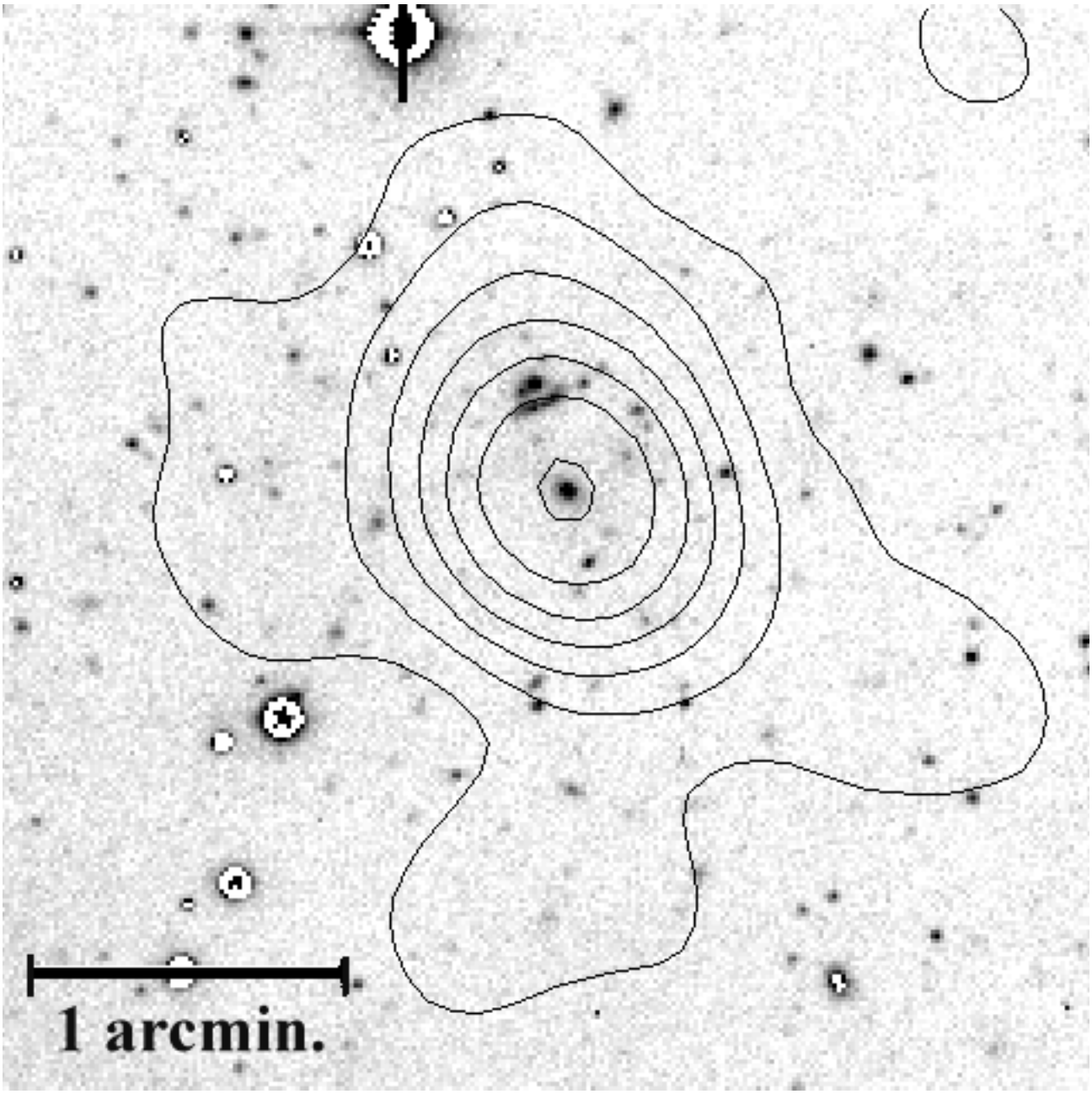


FIG. 2.—Significance contour plot of an X-ray image of AX J2239−0429 obtained by *ROSAT*/HRI (Trümper 1984). Subtracted background level is $1.25^{+0.05}_{-0.01} \times 10^{-6}$ counts s^{-1} arcsec^{-2}. The step size is 2 σ. The lowest contour level is 2 σ. This image is smoothed with a Gauss filter with a σ of 15″. Superposed is a $V + R$ image of Cl 2236−04 taken by the ESO 3.6 m (Melnick et al. 1993).

at $z = 0.552$ is $\sim 10\farcs6 = 78.4$ kpc. About 30% of the total emission detected by HRI is coming from the region within this cooling radius. Since the extent of the cooling flow is too small for the *ASCA* PSF to resolve the cooling flow region, and the photon statistics of the *ASCA* spectra of AX J2239−0429 are too poor to introduce any further parameters, the current *ASCA* spectra cannot constrain the cooling flow model.

TABLE 4

THE GAS MASS AND GRAVITATIONAL MASS OF AX J2239−0429 WITHIN 1.′4(0.6 h_{50}^{-1} Mpc) AND 1 h_{50}^{-1} Mpc

Parameter	0.6 h_{50}^{-1} Mpc	1.0 h_{50}^{-1} Mpc
n_{e_0} ($h_{50}^{1/2}$ cm^{-3})	2.44×10^{-2}	2.44×10^{-2}
$M_{\rm gas}$ ($h_{50}^{-5/2}$ $M_\odot$)	3.26×10^{13}	5.76×10^{13}
$M_{\rm grav}$ (h_{50}^{-1} $M_\odot$)	2.69×10^{14}	4.39×10^{14}
$M_{\rm gas}/M_{\rm grav}$ ($h_{50}^{-3/2}$)	0.12	0.13

3. COMPARISON WITH LENS MODELS

3.1. *Spherically Symmetric Lens Model*

First, we examine whether the cluster can be modeled by a spherically symmetric mass distribution. Assuming that the X-ray–emitting hot gas is isothermal and in hydrostatic equilibrium, the hydrostatic equilibrium equation gives the cluster mass contained within a radius r:

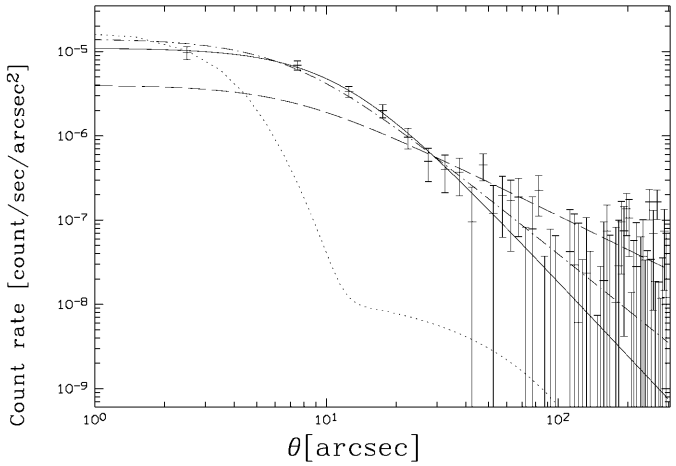


FIG. 3.—Background-subtracted radial surface brightness profile of AX J2239−0429 obtained from the *ROSAT*/HRI data. Errors are 1 σ, and the solid line is the best fit with the parameters shown in Table 3. The dotted line is a PSF profile at the X-ray peak. The best-fitting surface brightness model, assuming that the hot gas is isothermal—with the best-fit temperature (*dashed line*) and the 90% lower limit temperature for *ASCA* (*dashed-dotted line*)—and hydrostatic in the gravitational potential of the KMG model cluster, is also shown.

$$M(r) = \frac{kT}{G\mu m_{\rm H}} 3\beta \frac{r^3}{r_c^2} \frac{1}{1 + (r/r_c)^2}, \quad (2)$$

where $\mu = 1.3/2.1$ is the mean molecular weight for gas of cosmic abundance. Hereafter this model is referred to as the spherical isothermal β model. The lens equation for this mass distribution is

$$\tilde{\theta}_S = \tilde{\theta}_I - D \frac{\tilde{\theta}_I}{\sqrt{\tilde{\theta}_I^2 + 1}}, \quad (3)$$

where

$$D \equiv \frac{6\pi\beta}{\theta_c} \frac{kT}{\mu m_{\rm H} c^2} \frac{D_{LS}}{D_{OS}}, \quad (4)$$

$\tilde{\theta}_S$ ($\tilde{\theta}_I$) is the angle between the lens and the source (image) in units of θ_c, and D_{LS} (D_{OS}) is the angular diameter distance between the lens (the observer) and the source (the explicit expression is given in Fukugita et al. 1992). The value D is called the lens parameter and determines the efficiency of the lens. When $D \leq 1$, the lens always produces a single image, and image deformation is small. On the other hand, when $D > 1$, equation (2) has three routes for $\tilde{\theta}_S = 0$, such as

$$\tilde{\theta}_I = 0, \pm\sqrt{D^2 - 1}, \quad (5)$$

and an infinitely amplified circular image is formed with a radius of $(D^2 - 1)^{-1/2}\theta_c$, which is called the Einstein ring radius. The tangentially stretched giant luminous arc is formed near the tangential critical line in a spherical symmetric lens model. Therefore, a separation between the giant luminous arc and the center of the cluster must be close to the Einstein ring radius. Assuming that the giant luminous arc in Cl 2236−04 appears at the Einstein ring radius, the temperature and core radius measured by X-ray observations are compared in Figure 4 to a relation of those parameters required to explain the existence of the giant luminous arc at the observed position. If the universe does not contain a cosmological constant, a mass distribution

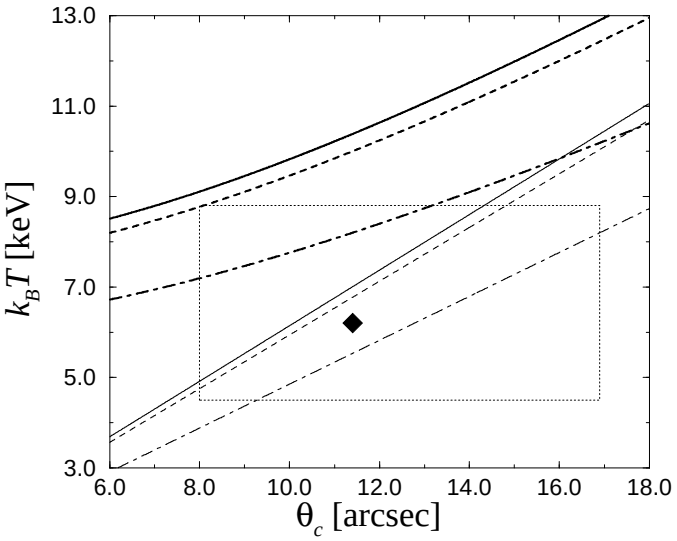


FIG. 4.—Comparison between the mass distribution derived from X-ray observations and that from a giant luminous arc. Bold lines show loci where the Einstein ring radii for the sources at $z = 1.116$ are equal to a separation between the giant luminous arc in Cl 2236−04 and the center of cD galaxy, that is, 12″.5, for various cosmological models. The solid line is for $(\Omega, \Lambda) = (1.0, 0)$, the dashed line is for $(\Omega, \Lambda) = (0.1, 0)$, and the dash-dotted line is for $(\Omega, \Lambda) = (0.1, 0.9)$, where the best-fit value is used for β and an isothermal spherical symmetric lens model is assumed. In each cosmological model, the Einstein ring radius is larger than 12″.5 in the region above the line. A region enclosed by 90% measurement error for temperature and core radius is shown by a dotted box. The best-fit values of temperature and core radius is shown by a diamond. As a reference, loci where the lens becomes critical, $D = 1$, are shown by thin lines for each cosmological model. At least the temperature and the core radius of the cluster must be in the region above these lines for the cluster to be able to make a strong lensing event for the sources at $z = 1.116$.

model derived from X-ray observations with a spherical isothermal β model cannot explain the existence of the giant luminous arc at the observed position, even if 90% one-parameter errors in temperature and core radius are taken into account. The observation of the giant luminous arc requires a higher temperature and smaller core radius; that is, it requires a stronger mass concentration in the cluster center than that derived from the X-ray observations. As shown in Figure 4, an introduction of a cosmological constant implies that a smaller mass concentration is able to reproduce the same Einstein ring radius compared to a zero cosmological constant model (e.g., Hamana et al. 1997). The temperature and core radius relation derived from the giant luminous arc position with $(\Omega_0, \Lambda_0) = (0.1, 0.9)$ has an overlapping region with a 90% error box obtained by X-ray observations.

3.2. *Nonspherical and Clumpy Lens Model*

There are several pieces of evidence indicating that deviations of the mass distribution in Cl 2236−04 from spherical symmetry are playing a significant role in the formation of the observed giant luminous arc. First of all, the almost straight nature of the giant luminous arc and the fact that no counterimage candidate has been found, in spite of a deep and wide field search (Kneib, Melnick, & Gopal-Krishna 1994, hereafter KMG), cannot be explained by a fold arc produced by a spherical symmetric lens. It implies either an elliptical or a substructural nature of the lens (Narasimha & Chitre 1993; KMG). Second, the X-ray morphology shows a clear deviation from a circular symmetry

and elongation in the northeast-southwest direction. Finally, there is a giant galaxy very close to the giant luminous arc, and a lensing effect by this galaxy should not be negligible.

Currently, the lens model proposed by KMG is the only successful model that is consistent with observed lensed image features. The model assumes two clumps of mass in this cluster. It predicts that the core radius (r_c) and the one-dimensional central velocity dispersion (σ_0) for the two clumps are $r_c = 7''$ (52 h_{50}^{-1} kpc) and $\sigma_0 = 610$ km s^{-1} for the clump centered on the cD galaxy and $r_c = 3''$ (22 h_{50}^{-1} kpc) and $\sigma_0 = 390$ km s^{-1} for the clump centered on the second giant galaxy in the cluster, where $H_0 = 50\ h_{50}$ km s^{-1} Mpc^{-1} and $\Omega_0 = 1$. The iso-mass densities of this model are shown in Figure 6 in KMG (note that south is up in the figure).

If a hydrostatic distribution for the X-ray–emitting gas is assumed (for validity of this assumption see, e.g., Schindler 1996), this lens mass model can be directly tested by X-ray observations. First of all, the coincidence between the X-ray peak and the cD center indicates that the center of cluster gravitational potential coincides with the cD position, as predicted by KMG. The core radius predicted by KMG is consistent with the *ROSAT*/HRI result within errors. The position angle of the X-ray image surprisingly coincides with the prediction of KMG. In the northern part of the cD galaxy, the direction of the major axis of the X-ray image is tilted northward. It might be evidence of a substructure in this direction (Neumann & Böhringer 1997), and it is roughly consistent with the position of the substructure predicted by KMG. In the limit of zero ellipticity, the lens equation of the cluster adopted by KMG (Mellier, Fort, & Kneib 1993) has the same functional form as equation (3). Since $\beta(kT/\mu m_{\rm H})/\theta_c$ in equation (3) ($\sim 5.5 \times 10^{14}$ cm^2 s^2 arcsec^{-1}) and the measured core radius are almost the same as σ_0^2/r_c in the KMG model ($\sim 5.3 \times 10^{14}$ cm^2 s^2 arcsec^{-1}) and KMG's core radius within the errors, the potential depth of the KMG model of cluster mass distribution is consistent with that inferred from the X-ray observations under assumptions of isothermal and hydrostatic equilibrium. In Figure 3, the best-fitting surface brightness model is shown, assuming that the hot gas is isothermal—with the best results for *ASCA* (*dashed line*) and the 90% lower limit for *ASCA* (*dashed-dotted line*)—and hydrostatic in the gravitational potential of the KMG model cluster with zero ellipticity and no substructure. In this fitting, only the central surface brightness is treated as a free-fitting parameter. Note that the three-dimensional cluster mass distribution is deduced as shown in Mellier et al. (1993) in this procedure. Although the model profile with the best-fit temperature is too flat, the profile with the 90% lower limit temperature gives a reasonably good fit, where the fitting result yields a χ^2 per degree of freedom of $73.65/59 = 1.25$. These results show that the KMG model is surprisingly consistent with the results of the X-ray observations.

4. DISCUSSIONS AND CONCLUSION

A new X-ray source in the direction of the distant lensing cluster, Cl 2236−04, is discovered by *ASCA*, named AX J2239−0429. The source extent is resolved by the following *ROSAT*/HRI observation, and it confirms that the X-ray source is the galaxy cluster Cl 2236−04.

The mass distribution of the cluster derived by X-ray observations and that derived by the observed nature of the giant luminous arc are compared. It is found that within the framework of a spherical isothermal β model, the mass required to explain the observed location of the giant luminous arc is larger than that expected from the X-ray observations, as reported for many giant luminous arc clusters (Wu & Fang 1997). An introduction of a large cosmological constant reduces the lensing mass, but the total reduction is only 20%–30%. Therefore, the cosmological constant cannot be the main solution for the discrepancy found in many clusters.

Cooling flow can be one of the other possible solutions (Allen et al. 1996; Allen 1998). According to the cooling flow model, the hot gas in the cluster central region is in the multitemperature phase. The temperature of the hottest phase gas, which represents a real gravitational potential depth, obtained by the multiphase model fitting becomes much higher than the temperature obtained by the single-phase model fitting, because the latter is the average temperature of the multitemperature gas. Allen (1998) claims that most of the discrepancy reported before can be explained by the existence of the cooling flow. There is much evidence of the existence of the cooling flow in the central region of AX J2239−0429, as shown in § 2. It may be possible that the measured temperature of AX J2239−0429 underestimates the cluster potential depth. If the *ASCA* temperature underestimates the cluster potential depth by a factor of 2 because of the cooling flow, the Einstein ring radius of the cluster for a source at $z = 1.116$ becomes as large as the distance between the giant luminous arc and the cluster center. However, the straight nature of the arc and the lack of a bright counterimage cannot be explained by a spherically symmetric lens. Further, the perturbation by the gravitational potential of galaxy A is not negligible. The absolute luminosity of galaxy A in the visual band is $3.3 \times 10^{11}\ h_{50}^{-2}\ L_\odot$ (Melnick et al. 1993). This luminosity is translated into the line-of-sight velocity dispersion of ~ 370 km s^{-1} by using the Faber-Jackson law (Binney & Tremaine 1987). If the potential depth is about a factor of 2 deeper than that inferred from the *ASCA* temperature, it is impossible to construct a model that is able to explain the location and the observed feature of the giant luminous arc because of the large perturbation of the galaxy A. Therefore we conclude that, even if the AX J2239−0429 has a cooling flow in the central region, the temperature measured by *ASCA*, which is the mean emission-weighted cluster temperature in this case, should not be different from the virial temperature of the cluster.

The most plausible solution is the effect of the clumpiness of the gravitational potential due to galaxy A and the nonzero ellipticity in the mass distribution of the cluster. KMG proposed the cluster mass distribution model by taking into account these effects, which explain the observed features of the giant luminous arc. The ellipticity, position angle, and velocity dispersion of the cluster predicted by KMG are surprisingly consistent with the results of the X-ray observations of the cluster, as shown in the previous section. The velocity dispersion of galaxy A assumed by KMG is also consistent with that deduced by the Faber-Jackson law. Therefore we conclude that the effect of the clumpiness of the gravitational potential due to galaxy A and the nonzero ellipticity in the mass distribution of the cluster are essential to explain the observed feature of the giant luminous arc, and the cluster mass distribution required by the strong lensing effect is totally consistent

with the X-ray observations, assuming that the X-ray–emitting hot gas is isothermal and in a hydrostatic equilibrium state.

The authors would like to thank J. Melnick, B. Altieri, Gopal-Krishna, and E. Giraud for providing the optical image of Cl 2236−04. M. H. and K. M. would like to thank Takashi Hamana and Mikio Murata for valuable discussions. M. H. is supported by the Yamada Science Foundation and by the Grants-in-Aid by the Ministry of Education, Science, and Culture of Japan (09740169, 60010500).

REFERENCES

Allen, S. W. 1998, in preperation (astro-ph/9710217)
Allen, S. W., Fabian, A. C., & Kneib, J.-P. 1996, MNRAS, 279, 615
Binney, J., & Tremaine, S. 1987, Galactic Dynamics (Princeton: Princeton Univ. Press)
Böhringer, H., Tanaka, Y., Mushotsky, R. F., Ikebe, Y., & Hattori, M. 1998, A&A, in press
Dickey, J. M., & Lockman, F. J. 1990, ARA&A, 28, 215
Fukugita, M., Futamase, T., Kasai, M., & Turner, E. L. 1992, ApJ, 393, 3
Hamana, T., Hattori, M., Ebeling, H., Henry, J. P., Futamase, T., & Shioya, Y. 1997, ApJ, 484, 574
Kneib, J.-P., Mellier, Y., Pelló, R., Miralda-Escudé, J., Le Borgne, J.-F., Böhringer, H., & Picat, J.-P. 1995, A&A, 303, 27
Kneib, J.-P., Melnick, J., & Gopal-Krishna. 1994, A&A, 290, L25 (KMG)
Loeb, A., & Mao, S. 1994, ApJ, 435, L109
Mellier, Y., Fort, B., & Kneib, J.-P. 1993, ApJ, 407, 33
Melnick, J., et al. 1993, A&A, 271, L5
Miralda-Escudé, J., & Babul, A. 1995, ApJ, 449, 18
Neumann, D. M., & Böhringer, H. 1997, MNRAS, 289, 123
Narasimha, D., & Chitre, S. M. 1993, A&A, 280, 57
Ota, N., Mitsuda, K., & Fukazawa, Y. 1998, ApJ, 495, 170
Piere, M., Le Borgne, L. F., Soucail, G., & Kneib, J.-P. 1996, A&A, 311, 413
Sarazin, C. L. 1986, Rev. Mod. Phys., 58, 1
Schindler, S. 1996, A&A, 305, 756
Schindler, S., Hattori, M., Neumann, D. M., & Böhringer, H. 1997, A&A, 317, 646
Schindler, S., et al. 1995, A&A, 299, L9
Takahashi, T., et al. 1995, *ASCA* News 3, NASA/GSFC, 34
Tanaka, Y., Inoue, H., & Holt, S. S. 1994, PASJ, 46, L37
Trümper, J. E. 1984, Phys. Scr., T7, 209
Wu, X. P., & Fang, L. Z. 1997, ApJ, 483, 62